Dalton Transactions

PAPER

View Article Online
View Journal | View Issue

Cite this: *Dalton Trans.*, 2019, **48**, 117

[Ge(Te^{n}Bu)$_4$] – a single source precursor for the chemical vapour deposition of germanium telluride thin films†

Samantha L. Hawken,[a] Ruomeng Huang,[b] C. H. (Kees) de Groot,[b] Andrew L. Hector,[a] Marek Jura,[c] William Levason,[a] Gillian Reid *[a] and Gavin B. G. Stenning[c]

Received 9th August 2018,
Accepted 4th October 2018

DOI: 10.1039/c8dt03263g

rsc.li/dalton

Reaction of activated germanium with ^{n}Bu$_2$Te$_2$ in THF solution was shown to be more effective for the preparation of the germanium(IV) tellurolate compound, [Ge(Te^{n}Bu)$_4$], than reaction of GeCl$_4$ with LiTe^{n}Bu in a 1 : 4 molar ratio in THF. The product was characterised by ^{1}H, ^{13}C{^{1}H} NMR spectroscopy and microanalysis and evaluated as a single source precursor for the low pressure chemical vapour deposition of GeTe thin films. Depending upon deposition conditions, either dull grey films (predominantly elemental Te) or highly reflective (GeTe) films were obtained from the pure precursor. Grazing incidence X-ray diffraction shows that the highly reflective films are comprised of the rhombohedral α-GeTe phase, while scanning electron microscopy and energy dispersive X-ray analysis reveal rhomb-shaped crystallites with a 49(1) : 51(1)% Ge : Te ratio. This structure is also confirmed from Raman spectra. Van der Pauw measurements show ρ = 3.2(1) × 10^{-4} Ω cm and Hall electrical measurements indicate that the GeTe thin films are p-type, with a mobility of 8.4(7) cm^2 V^{-1} s^{-1} and carrier concentration of 2.5(2) × 10^{21} cm^{-3}. The high p-type concentration is most likely a result of the substantial Ge vacancies in its sub-lattice, in line with the EDX elemental ratios.

Introduction

The binary IV–VI semiconductor, GeTe, is a promising candidate for a number of technologically important applications,[1] including for incorporation into thermoelectric,[2,3] ferroelectric[4] and spintronic materials,[5–7] as well as in solid state memory,[8,9] where GeTe is layered alternately with Sb_2Te_3 [10] in interfacial memory or combined with Sb_2Te_3 in the ternary $Ge_2Sb_2Te_5$ (GST-225) alloy.[8,9] Its phase change memory applications arise since GeTe has a highly conductive crystalline state, whilst in the amorphous phase it is highly resistive.[11] It also exhibits extremely fast switching speeds, as low as 1 ns.[12]

GeTe is one of the best known p-type thermoelectric materials. However, its relatively low Seebeck coefficient (~30 μV K^{-1}) due to large p-type carrier concentrations (~10^{21} cm^{-3}) has largely affected its thermoelectric properties, leading to a maximum ZT value of 0.7 at 720 K.[13] Recently, GeTe-rich alloys such as Ge–Pb–Te, Ge–Sb–Te and GeTe-$AgSbTe_2$ have demonstrated enhanced thermoelectric performance and have generated great interest in further investigating GeTe-based alloys for intermediate temperature thermoelectric applications.[14]

Crystalline germanium telluride can adopt three distinct phases, α-GeTe, β-GeTe and γ-GeTe.[1,15] β-GeTe has a rocksalt structure ($Fm\bar{3}m$), and is found only above 630 K.[15,16] At lower temperature GeTe exists either in the rhombohedral, distorted rocksalt structure (α-GeTe, $R\bar{3}m$) or the orthorhombic structure (γ-GeTe), with the orthorhombic structure prevalent at Te > 51.2%.[15] It is the Peierls effect that causes the distortion in the rocksalt structure to form α-GeTe and has important implications in GeTe based phase change memory.[17] The outcome is alternating short strong and long weak GeTe bonds aligned in the (111) plane, causing the unit cell to become elongated in this direction.[18,19]

Various forms and morphologies of GeTe have been deposited using a range of techniques. GeTe nanowires and single crystals have been grown by vapour liquid solid growth,[20,21] while thin films have mostly been produced by sputtering[22,23] and molecular beam epitaxy.[24,25] Other techniques, including thermal co-evaporation[26] and atomic layer

[a]School of Chemistry, University of Southampton, Southampton SO17 1BJ, UK. E-mail: G.Reid@soton.ac.uk
[b]School of Electronics and Computer Science, University of Southampton, Southampton SO17 1BJ, UK
[c]ISIS Neutron and Muon Source, Rutherford Appleton Laboratory, Harwell Science and Innovation Campus, Didcot, OX11 0QX, UK

†Electronic supplementary information (ESI) available: Spectroscopic data for the product from Method 2, GIXRD data for a film from Method 1 containing both GeTe and Te. See DOI: 10.1039/c8dt03263g

deposition (using $\{(CH_3)_3Si\}_2Te$ and either $HGeCl_3$ or $Ge\{N[Si(CH_3)_3]_2\}_2$) have also been employed.[27] GeTe nanocrystals have also been synthesised from $GeCl_2$·dioxane or $Ge\{N[Si(CH_3)_3]_2\}_2$ with trioctyl phosphine telluride.[28]

Chemical vapour deposition (CVD) is a widely used deposition technique for thin films and coatings, with its relatively low cost and scalability being particular attractions, while, unlike PVD, it is not a line-of-sight technique.[29] Dual source CVD has been used for the growth of GeTe thin films.[30,31] For example, Salicio *et al.* used $Ge(NMe_2)_4$ and Te^iPr_2 in toluene in a pulsed liquid injection CVD method to produce Te-rich GeTe films ($Ge_{0.79}Te_{1.00}$).[30] For the heavier group 14 metal chalcogenides, SnE_2 and SnE (E = S, Se, Te), a range of single source precursors have been developed to deposit either the tin mono- or di-chalcogenide thin film through judicious choice of precursor and/or deposition conditions, *e.g.* $[Sn(SCH_2CH_2S)_2]$,[32] various alkyl tin dithiocarbamates,[33] thio/selenoether complexes of $SnCl_4$ [34,35] and tin chalcogenide guanadinato complexes.[36] As well as offering increased control of stoichiometry, using single source precursors can offer the added advantage of selective deposition of the binary material onto specific regions of a (lithographically) patterned substrate, as demonstrated for example with Sn(IV) chloride complexes bearing neutral chalcogenoether ligands, such as $[SnCl_4\{^nBuE(CH_2)_nE^nBu\}]$ (n = 2, 3).[35] This selectivity can be beneficial for particular applications.

However, the lighter $GeCl_4$ is an extremely weak Lewis acid and consequently, complexes of Ge(IV) chloride with neutral chalcogenoether ligands do not exist. Using the more Lewis acidic GeF_4, a small number of coordination complexes with neutral dithioethers has been reported, $[GeF_4\{MeS(CH_2)_2SMe\}]$ and $[GeF_4\{EtS(CH_2)_2SEt\}]$. Whilst crystallographic data confirm their distorted octahedral structures, these complexes are very labile, with weak (long) Ge–S bonds,[37] and analogues containing the less basic selenoether/telluroether ligands do not seem to be accessible.

A small number of single source precursors for the deposition of GeTe crystals are reported in the literature, although, with one exception (below), these have not been used for the CVD of GeTe thin films. Gupta *et al.* synthesised $(R_2GeTe)_3$ (R = Et, Bu) (**1**) from the reaction of Li_2Te and R_2GeCl_2, and thermal decomposition of the precursor in trioctylphosphine at 300 °C resulted in rhombohedral GeTe,[38] while Kim *et al.* showed that thermal decomposition of [Te = Ge(dmampS)$_2$] (**2**) in hexadecane at 270 °C produced Te-rich rhombohedral $Ge_{40}Te_{57}$.[39]

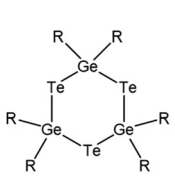

(1)

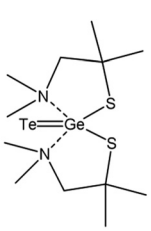

(2)

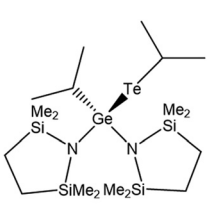

(3)

There is just one previous example of a single source CVD precursor for the deposition of GeTe thin films. Using $[Ge\{N(SiMe_2CH_2CH_2Me_2Si)\}_2(^iPr)(Te^iPr)]$ (**3**) in NH_3, Chen *et al.* reported that GeTe film growth occurs between 280 and 400 °C.[40] However, characterisation data reported on the resulting materials was limited.

In view of the technologically important applications of GeTe thin films and the paucity of single source precursors for CVD of high quality GeTe films, we report here the development and characterisation of $[Ge(Te^nBu)_4]$ and application of this compound as a single source precursor for the low pressure CVD of highly reflective, crystalline GeTe thin films. Grazing incidence X-ray diffraction (GIXRD), scanning electron microscopy (SEM), energy dispersive X-ray (EDX) and Raman analyses to establish the structural and compositional characteristics of the films, as well as electrical characterisation *via* van der Pauw and Hall measurements, are discussed.

Results and discussion

Precursor synthesis

Due to the extremely weak Lewis acidity of $GeCl_4$ and the complete absence of any telluroether complexes of germanium in the literature, coordination complexes suitable for use as single source precursors for germanium telluride thin films are not accessible. However, compounds such as the antimony chalcogenolates $[Me_xSb(E^nBu)_{3-x}]$ (E = Se, Te), have previously been synthesised by the direct reaction of LiE^nBu with $1/(3-x)$ Me_xSbCl_{3-x}. For x = 0 or 1, these were shown to function as efficient single source precursors for the deposition of Sb_2E_3 thin films.[41] Consequently, the compound, $[Ge(Te^nBu)_4]$ was identified as a possible precursor for GeTe thin film deposition. Two methods were explored for the synthesis of this compound, as illustrated in Scheme 1.

Method 1 afforded the product as a viscous dark red oil. Characterisation by ^1H and $^{13}C\{^1H\}$ NMR spectroscopy were consistent with formation of the desired $[Ge(Te^nBu)_4]$ product, together with variable amounts of $^nBu_2Te$ and $^nBu_2Te_2$ ($^{13}C\{^1H\}$ and $^{125}Te\{^1H\}$ NMR evidence). Attempts to separate this mixture by placing it under vacuum, or by distillation, were unsuccessful. Attempts to optimise the synthesis of $[Ge(Te^nBu)_4]$ using Method 1 by adjusting the reaction temperature, reaction times and ^{n}BuLi : Te ratio, met with some success, although small amounts of the same Te by-products were always evident, hence an alternative synthesis for this precursor was sought.

Schlecht *et al.* reported the synthesis of $[Ge(EPh)_4]$ (E = Se, Te) by the reaction of activated germanium with Ph_2E_2 (E = Se, Te).[42] Whilst the selenolate derivative was produced in good yield, the germanium tellurolate compound was afforded in only 26% yield. We replicated this synthesis, resulting in a mixture of Ph_2Te_2 and $[Ge(TePh)_4]$ in a ~40 : 60 ratio. Separation of the products was achieved by washing the product with ice cold diethyl ether, although this reduced the isolated yield significantly.

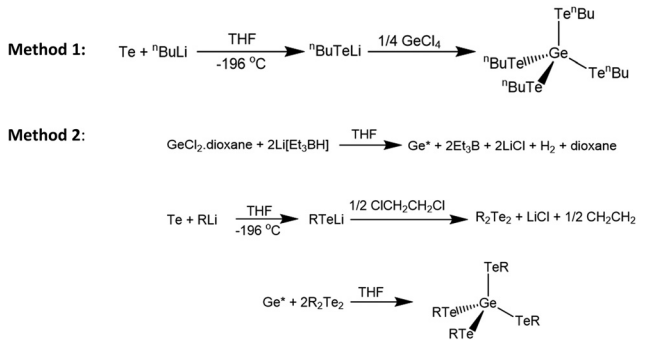

Scheme 1 Methods employed for the synthesis of $[Ge(Te^nBu)_4]$.

In order to obtain a pure sample of the target CVD precursor, $[Ge(Te^nBu)_4]$, the method was adapted (Method 2), using $^nBu_2Te_2$ in place of Ph_2Te_2. The $^nBu_2Te_2$ was first synthesised *via* the reaction of ^{n}BuTeLi with 1,2-dichloroethane. 1,2-Bis(butyltelluro)ethane is unstable and decomposes spontaneously to form $^nBu_2Te_2$ with elimination of ethene. The resulting $^nBu_2Te_2$ is a dark red oil and was stored under nitrogen in the freezer. The isolated material was spectroscopically pure by ^{1}H, $^{13}C\{^1H\}$ and $^{125}Te\{^1H\}$ NMR analysis.

As the target $[Ge(Te^nBu)_4]$ is an oil, it was expected that separation of this from $^nBu_2Te_2$ would be more difficult than for the solid $[Ge(TePh)_4]$. It is not possible to know the actual yield of Ge*, however, it can be assumed that the yield of Ge* is not 100%, and therefore a deficit of $^nBu_2Te_2$ is required for the synthesis to minimise the amount of unreacted $^nBu_2Te_2$ present in the final product. We found that using only half of the stoichiometric amount of $^nBu_2Te_2$ in Method 2 resulted, after work-up, in the formation of a dark red oil whose microanalysis was consistent with the proposed $[Ge(Te^nBu)_4]$ formulation. Characterisation by ^{1}H and $^{13}C\{^1H\}$ NMR spectroscopy also showed that the desired product had been obtained without any $^nBu_2Te_2$ or $^nBu_2Te$ by-products, (Table 1, Fig. S1 and S2†). IR spectroscopy showed bands at 238 and 251 cm^{-1}. The former is tentatively assigned to the Ge–Te stretching vibration. Thus, Method 2 appears to provide a more effective for the preparation of pure $[Ge(Te^nBu)_4]$.

Monitoring a $CDCl_3$ solution of the $[Ge(Te^nBu)_4]$ by ^{1}H NMR spectroscopy showed that it decomposes slowly over time, producing $^nBu_2Te_2$. This decomposition was much slower when the $[Ge(Te^nBu)_4]$ was stored under a dry N_2 atmosphere in the freezer.

Table 1 $^{13}C\{^1H\}$ NMR data for $[Ge(Te^nBu)_4]$ and the main potential organotellurium by-products ($CDCl_3$)

Compound	$\delta(^{13}C)$/ppm			
$[Ge(Te^nBu)_4]$	12.90	13.53	25.29	34.53
$^nBu_2Te$	2.24	13.33	25.03	34.32
$^nBu_2Te_2$	4.22	13.32	24.56	35.72

Low pressure CVD of GeTe thin films

Low pressure CVD experiments were undertaken using the precursor produced from both Methods 1 and 2. A typical experiment used ~50 mg of precursor and PVD SiO_2 on Si substrates. Low pressure CVD using the precursor obtained *via* Method 1 resulted in partial evaporation of the precursor, with some black residue remaining. Deposition occurred onto the substrate closest to the precursor, producing a silvery, very reflective film, while at the edge of the film closest to the precursor, the deposit was a dull grey.

Grazing incidence X-ray diffraction (XRD) analysis, as shown in Fig. 1, revealed that the reflective film was phase pure rhombohedral (α-GeTe), with space group *R3mH*. Refined lattice parameters (a = 4.145(2), c = 10.620(8) Å) are consistent with those reported in the literature (a = 4.156(3), c = 10.663(5);[43] a = 4.164 (2), c = 10.69(4)).[44] Crystallite sizes were estimated from the diffraction data peak widths at ~200 nm. An enhancement to the intensity of the 003 reflection (0.3× the intensity of the 02–2 compared with 0.06× in the standard pattern) suggests some preferred orientation of this axis of the crystallites to the substrate surface normal. This is not seen in the higher angle 006 peak, as expected, since in grazing incidence geometry the diffraction vector of this peak is inclined further from the surface normal and would be less affected by this crystallite preferred orientation. Further, the dull grey region was shown by XRD to be formed of a mixture of GeTe and crystalline tellurium (Fig. S3†).

Scanning electron microscopy (SEM) analysis of the GeTe film revealed a uniform array of crystallites. The film also appears to be very smooth, and therefore reflective. A cross sectional SEM image shows that the film has a thickness of ~100 nm (Fig. 2). This is smaller than the crystallite size indicated from the diffraction data and, combined with the observed preferred orientation, it is likely that the crystallites have a tendency to grow as platelets in the a/b plane as observed in the thicker films (Fig. 5).

Energy dispersive X-ray (EDX) analysis showed the Ge : Te ratio was 49(1) : 51(1), with no impurities detected (Fig. 3a). GeTe is often found in an imperfect stoichiometry due to intrinsic point defects (dominated by Ge vacancies).[46,47] The Raman spectrum from the film (Fig. 3b) shows three peaks at

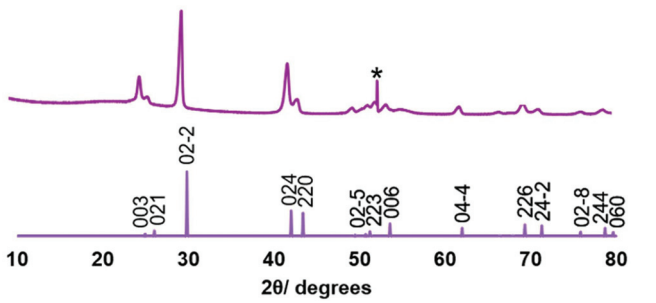

Fig. 1 XRD pattern obtained for the GeTe film deposited on PVD SiO_2 from $[Ge(Te^nBu)_4]$ synthesised *via* Method 1 (top) and an indexed literature XRD pattern for bulk GeTe (bottom).[45] The peak due to the Si underlying the SiO_2 in the substrate is marked *.

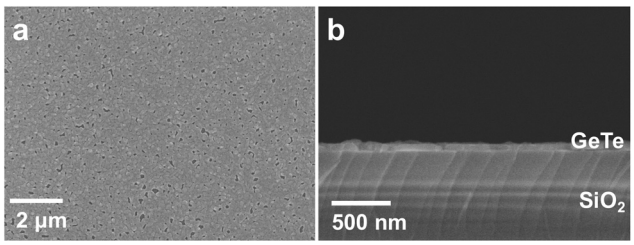

Fig. 2 Top view (a) and cross section (b) SEM images of a GeTe film deposited onto PVD SiO_2 from $[Ge(Te^nBu)_4]$ synthesised by Method 1.

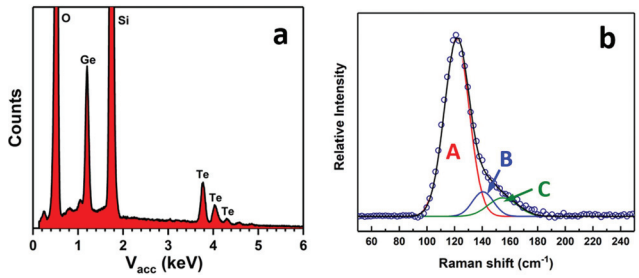

Fig. 3 EDX spectrum (a) and Raman spectrum (b) from a GeTe film deposited onto PVD SiO_2 using $[Ge(Te^nBu)_4]$ prepared *via* Method 1.

~122 cm^{-1}, ~140 cm^{-1} and ~155 cm^{-1}, which is consistent with those reported in the literature.[25,48–50] Peak A at ~122 cm^{-1} can be assigned to the symmetric stretching vibrations of $GeTe_4$ tetrahedra (A_{1g}) and peak C, at ~155 cm^{-1}, corresponds to the vibrations of Ge atoms distinct from their distorted octahedral sites. The additional peak at ~140 cm^{-1} (B) potentially originates from the aging effect.[50,51]

The resistivity of the GeTe film was determined by van der Pauw measurements, giving $\rho = 3.2(1) \times 10^{-4}$ Ω cm, which compares well with other reported values ($\rho = 1.4 \times 10^{-4}$ Ω cm).[13] Hall measurements revealed that the GeTe film is a p-type semiconductor with a mobility of 8.4(7) $cm^2\ V^{-1}\ s^{-1}$ and carrier concentration of $2.5(2) \times 10^{21}$ cm^{-3}. This high p-type concentration is a result of the substantial Ge vacancies in its sub-lattice, as also suggested by the EDX results.[52]

Since it proved difficult to obtain GeTe films using the precursor from Method 1 without co-deposition of elemental Te, CVD experiments were performed under similar conditions using the pure $[Ge(Te^nBu)_4]$ compound obtained *via* Method 2. These also led to partial evaporation of the precursor with some black residue remaining. Good coverage of the substrates was observed, with dull grey films on the two substrates nearest the precursor (cooler region, substrate T ~300–330 °C), shown to be dominated by elemental Te, while films that were deposited further into the hot zone were highly reflective and silver in colour. Characterisation of the latter (substrate T ~360–400 °C) by grazing incidence XRD showed that only rhombohedral GeTe was present (space group *R3mH*), with no trace of crystalline tellurium (Fig. 4). Lattice parameters (a = 4.1565(10), c = 10.646(3) Å) also match well with the literature

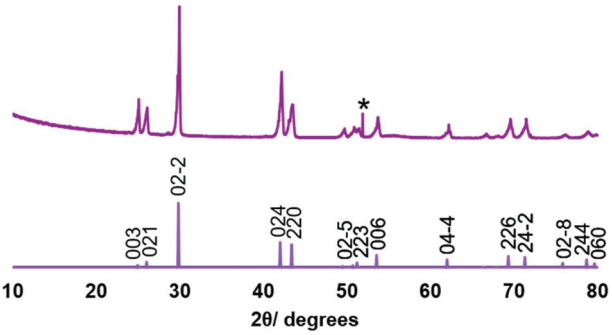

Fig. 4 XRD pattern obtained for the GeTe film deposited on PVD SiO_2 from $[Ge(Te^nBu)_4]$ synthesised *via* Method 2 (top) and an indexed literature XRD pattern for bulk GeTe (bottom).[53] The peak due to the Si underlying the SiO_2 in the substrate is marked *.

data.[41,42] We note that low pressure CVD experiments using $[Ge(TePh)_4]$ did not result in any significant film deposition, likely due to a combination of the stronger Te–C(aryl) bonds, the lower volatility of this compound, coupled with the its inability to undergo a low energy decomposition pathway, such as β-hydride elimination.

SEM analysis (Fig. 5) shows much larger crystallites (~1–2 microns in diameter) than those in the film deposited from the precursor from Method 1. The film is around 1.5–2 μm thick, in line with the typical crystallite dimensions.

EDX analysis revealed both germanium and tellurium to be present, with no indication of any residual carbon (K_α = 0.277 keV), as shown in Fig. 6a. Quantification of the germa-

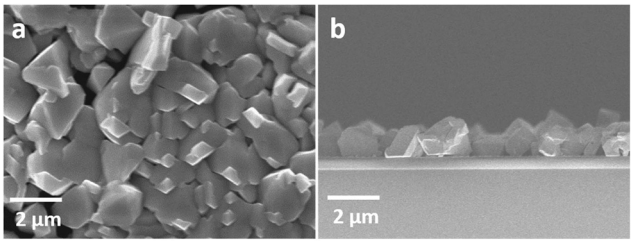

Fig. 5 Top view (a) and cross section (b) SEM images of a GeTe film deposited onto PVD SiO_2 from $[Ge(Te^nBu)_4]$ synthesised *via* Method 2.

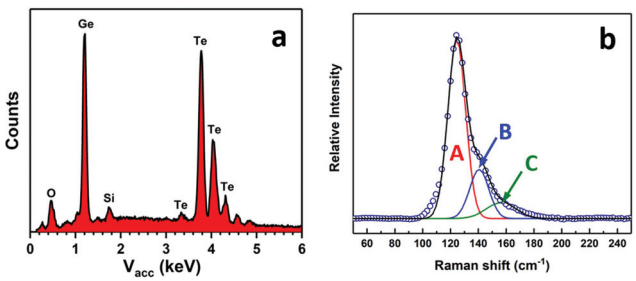

Fig. 6 EDX analysis (a) and Raman spectrum (b) from a GeTe film deposited onto PVD SiO_2 from $[Ge(Te^nBu)_4]$ prepared *via* Method 2.

nium and tellurium peaks gave a ratio of 49(1) : 51(1) Ge : Te. Raman spectra from the films (Fig. 6b) also show three peaks positioned at ~124 cm^{-1}, ~141 cm^{-1} and ~156 cm^{-1}. The slight upshift of the phonon modes compared with that in Fig. 3 can be ascribed to the increase of the crystal size which also leads to peak narrowing of the Raman spectra.[48] The discontinuity of the films obtained using the precursor from Method 2 precluded electrical measurements.

Experimental

IR spectra were recorded as Nujol mulls or neat thin films between CsI plates using a PerkinElmer Spectrum 100 instrument over the range 4000–200 cm^{-1}. ^{1}H and $^{13}C\{^{1}H\}$ NMR spectra were recorded from solutions in $CDCl_3$ or CD_2Cl_2 on a Bruker AV400 spectrometer and referenced to TMS *via* the residual protio-solvent resonance. $^{125}Te\{^{1}H\}$ NMR spectra were recorded from solutions in CD_2Cl_2 on a Bruker AV400 spectrometer and referenced to external neat $TeMe_2$. Microanalytical results were obtained from Medac Ltd.

Substrate preparation

PVD SiO_2 films with a thickness of either 500 nm or 1 μm were deposited on silicon wafers by the medium frequency magnetron sputtering method using a pure Si (99.99% purity) target with a DC power of 2000 W in an O_2/Ar atmosphere. The O_2 and Ar flow rates were maintained at 20 and 40 SCCM respectively. With a drive speed of 180 rpm, the deposition rate was 0.3 nm s^{-1}.

Thin film characterisation

Grazing incidence X-ray diffraction patterns were collected using a Rigaku SmartLab system, with CuK_α X-rays, a 2θ scan range of 10–80° and an incident angle of 1°. The XRD patterns were matched to literature patterns to determine the crystalline phase.[54] Lattice parameters were calculated by optimisation of the fit of grazing incidence or in plane XRD patterns in PDXL2.[55] Scanning electron microscopy (SEM) images and energy dispersive X-ray (EDX) measurements were obtained using a JEOL JSM 6500 F Field Emission Scanning Electron Microscope with an Oxford INCA x-sight 7418 EDX probe. An accelerating voltage of 10 or 15 kV was used. High resolution cross sectional SEM images were obtained using a field emission SEM (Jeol JSM 7500F) at an accelerating voltage of 5 kV. Raman scattering spectra were measured at room temperature on a Renishaw InVia Micro Raman Spectrometer using a helium–neon laser with a wave-length of 632.8 nm. The incident laser power was adjusted to 0.1 mW for all samples. Van der Pauw measurements were performed at room temperature on a Nanometrics HL5500PC at 300 K. For each measurement, four copper probes with diameter of *ca.* 1 mm were carefully placed on the sample corners. Extra care was taken to ensure linear contact was obtained between each probe and the sample before each measurement.

$^{n}Bu_2Te_2$. Freshly ground Te powder (6.40 g, 0.05 mol) was suspended in anhydrous THF (100 mL) and frozen at −196 °C in liquid nitrogen. ^{n}BuLi (1.6 M, 31.3 mL, 0.05 mol) was added slowly. The mixture was allowed to thaw to form a dark red solution. It was then cooled on ice and a further small aliquot of ^{n}BuLi was added dropwise until a pale yellow solution was formed. This was again frozen in liquid nitrogen and 1,2-dichloroethane (2 mL, 0.025 mol) was added. The reaction mixture was allowed to thaw and stirred for 1 h to afford a red solution. The solvent was removed *in vacuo* and the product was extracted with anhydrous CH_2Cl_2 and washed with degassed water. Following separation, the CH_2Cl_2 extract was dried ($MgSO_4$), and the solvent was removed *in vacuo* to leave a red oil (7.77 g, 64%). ^{1}H NMR ($CDCl_3$, 298 K): δ/ppm = 0.94 (t, [3H], CH_3), 1.40 (m, [2H], CH_2), 1.72 (m, [2H], CH_2), 3.12 (m, [2H], $TeCH_2$). $^{13}C\{^{1}H\}$ NMR ($CDCl_3$, 298 K): δ/ppm = 4.22, 13.32, 24.56, 35.72. $^{125}Te\{^{1}H\}$ NMR ($CDCl_3$, 298 K): δ/ppm = 112.9 ppm.

[Ge(Te^{n}Bu)$_4$] – Method 1. Te powder (3.23 g, 25.0 mmol) was suspended in anhydrous THF (100 mL) and this was frozen in liquid N_2 (−196 °C). ^{n}BuLi (1.6 M, 16.4 mL, 25.0 mmol) was added slowly. The solution was allowed to thaw and was stirred for 2 h. A dark brown solution was formed. $GeCl_4$ (0.723 mL, 6.33 mmol) in anhydrous THF (10 mL) was added and the solution was allowed to stir for 16 h. The solvent was removed *in vacuo* to leave a dark brown solid. This was extracted with anhydrous CH_2Cl_2 and filtered. The filtrate was a bright red solution. The solvent was removed *in vacuo* to leave a red viscous oil that was stored in the freezer. ^{1}H NMR ($CDCl_3$, 298 K): δ/ppm [Ge(Te^{n}Bu)$_4$]: 0.93 (t, [3H], CH_3), 1.42 (m, [2H], CH_2), 1.86 (m, [2H], CH_2), 2.79 (m, [2H], $TeCH_2$), $^{n}Bu_2Te$: 0.93 (t, [3H], CH_3), 1.42 (m, [2H], CH_2), 1.86 (m, [2H], CH_2), 2.63 (m, [2H], $TeCH_2$), $^{n}Bu_2Te_2$: 0.93 (t, [3H], CH_3), 1.42 (m, [2H], CH_2), 1.86 (m, [2H], CH_2), 3.11 (m, [2H], $TeCH_2$). $^{13}C\{^{1}H\}$ NMR ($CDCl_3$, 298 K): δ/ppm [Ge(Te^{n}Bu)$_4$]: 13.33, 13.66, 25.69, 35.18, $^{n}Bu_2Te$: 2.54, 13.33, 25.12, 35.07, $^{n}Bu_2Te_2$: 4.67, 13.87, 25.86, 36.32 IR (neat film) ν/cm^{-1}: 238 (Ge–Te).

[Ge(TePh)$_4$]. Synthesised according to the literature method.[42] [$GeCl_2$(dioxane)] (232 mg, 1.0 mmol) was dissolved in anhydrous THF (50 mL). It was reduced with $Li(Et_3BH)$ (1 M, 2 mL). Once H_2 evolution had ceased, the solution was decanted, and the precipitated Ge was washed with anhydrous THF (3 × 50 mL). It was then suspended in anhydrous THF (60 mL) and Ph_2Te_2 (818 mg, 2.0 mmol) was added. This reaction mixture was stirred at room temperature for 2 h to form a red solution. The THF was removed *in vacuo* and the remaining solid was dissolved in anhydrous diethyl ether (50 mL) and filtered. The filtrate was evacuated to dryness and washed with ice cold diethyl ether (3 × 5 mL) to afford a bright red solid. ^{1}H NMR ($CDCl_3$, 298 K): δ/ppm [Ge(TePh)$_4$]: 7.19 (m, [8H]), 7.38 (m, [4H]), 7.60 (m, [8H],); Ph_2Te_2: 7.24 (m), 7.80 (m) (~60 : 40 ratio).

[Ge(Te^{n}Bu)$_4$] – Method 2. [$GeCl_2$(dioxane)] (464 mg, 2.00 mmol) was dissolved in anhydrous THF (100 mL) and it was reduced by addition of $Li[Et_3BH]$ (4.00 mL, 4.00 mmol). A yellow orange precipitate was formed. The THF was decanted and the activated Ge residue was washed with anhydrous THF (3 × 50 mL). It was then suspended in anhydrous THF (50 mL)

and $^{n}Bu_2Te_2$ (0.488 g, 2.00 mmol) in anhydrous THF (10 mL) was added and the solution left to stir under N_2 for 3 h. The THF was removed *in vacuo*. The residue was extracted with anhydrous diethyl ether and filtered. The solvent was removed *in vacuo* to afford a dark red oil. ^{1}H NMR ($CDCl_3$, 298 K): δ/ppm: 0.94 (t, [3H], CH_3), 1.43 (m, [2H], CH_2), 1.87 (m, [2H], CH_2), 2.79 (m, [2H], $TeCH_2$). $^{13}C\{^{1}H\}$ NMR ($CDCl_3$, 298 K): δ/ppm: 12.90, 13.53, 25.29, 34.53. $^{125}Te\{^{1}H\}$ NMR ($CDCl_3$, 298 K, 190 K): δ/ppm: no signal observed. IR (neat thin film) ν/cm^{-1}: 238 (Ge–Te). Anal. calcd for $C_{16}H_{36}GeTe_4$: C 23.68, H 4.47; found: C 24.32, H 4.77%.

Low pressure CVD experiments

Typical experiments involved loading *ca.* 50 mg of the neat precursor into the closed end of a silica tube in a dry, N_2-filled glove box. Six PVD SiO_2 coated substrate tiles (each 20 × 8 × 1 mm^3) were then placed end-to-end lengthways along the tube from the end nearest the precursor. The N_2-filled tube was then closed with a tap, placed horizontally in a Lenton tube furnace (total length = 36 cm, of which the central 30 cm is heated) and connected to a vacuum line. The tube was positioned such that the precursor was ~2 cm outside the furnace and then evacuated to 0.02 mm Hg. The furnace was set to 450 °C. Once the temperature across the tube had stabilised, the tube was repositioned such that the precursor was placed at the edge of the furnace and heating was maintained until precursor evaporation was observed (220–240 °C). Evaporation was typically complete within 15–20 min. Following this, the furnace was cooled to room temperature, and the tube was filled with N_2 before being transferred to the glove box and the substrates were unloaded.

Conclusions and outlook

Two alternative methods for the preparation of $[Ge(Te^{n}Bu)_4]$ have been developed, with Method 2 yielding the product in higher purity and in better yield compared to Method 1, which tended to also produce a significant amount of $^{n}Bu_2Te_2$ and $^{n}Bu_2Te$ by-products that could not be separated. The $[Ge(Te^{n}Bu)_4]$ has been evaluated for the low pressure CVD of GeTe thin films, providing an effective single source CVD precursor for this technologically important material. The α-GeTe phase present in the thin films produced from the $[Ge(Te^{n}Bu)_4]$ precursor obtained from both methods has been identified by grazing incidence XRD, SEM, EDX and Raman spectroscopy. The only significant difference in the deposited films is the morphology of the GeTe grown using the precursor from Method 2, which is comprised of much larger crystallites (and hence less continuous). The precursor from Method 1 led to thinner, more continuous films, most likely as a result of being formed of much smaller crystallites. The measured resistivity for the latter, determined by van der Pauw measurements, compares well with the values determined for sputtered GeTe. While the single source GeTe precursor decomposes slowly over time, it can be stored for several months in the freezer (−18 °C). The presence of a 1 : 4 Ge : Te ratio in the precursor compound also results in co-deposition of elemental Te in some of the films obtained at lower temperatures. It is likely that modification of the precursor to a 1 : 1 Ge : Te ratio, for example using compounds of the form $[R_3GeTe^{n}Bu]$, would eliminate (or reduce) the Te co-deposition, further enhancing the precursor properties for GeTe film growth and allowing even better control of film morphology. Looking forward, by combining this precursor with $MeSb(Te^{n}Bu)_2$ it may be possible to deposit $Ge_2Sb_2Te_5$ (GST-225) for phase change memory applications, or alternating layers of $GeTe/Sb_2Te_3$ for interfacial memory. The latter is particularly attractive as it has been shown to have faster switching times than GST-225, as low as 10 ns, and these superlattices have also shown increased write/erase lifetimes when used in data storage applications.[14,15] This will be the focus of our future work.

Conflicts of interest

There are no conflicts to declare.

Acknowledgements

We thank the STFC for funding (ST/P00007X/1) and for an EPSRC Case Award to S. L. H. (EP/M50662X/1). We also gratefully acknowledge funding for thin film diffraction and NMR instrumentation from the EPSRC through EP/K00509X, EP/K009877/1 and EP/K039466/1.

References

1 J. E. Boschker, R. Wang and R. Calarco, *CrystEngComm*, 2017, **19**, 5324–5335.
2 C. Wood, *Rep. Prog. Phys.*, 1988, **51**, 459–539.
3 D. Wu, L.-D. Zhao, S. Hao, Q. Jiang, F. Zheng, J. W. Doak, H. Wu, H. Chi, Y. Gelbstein, C. Uher, C. Wolverton, M. Kanatzidis and J. He, *J. Am. Chem. Soc.*, 2014, **136**, 11412–11419.
4 M. J. Polking, M. G. Han, A. Yourdkhani, V. Petkov, C. F. Kisielowski, V. V. Volkov, Y. Zhu, G. Caruntu, A. P. Alivisatos and R. Ramesh, *Nat. Mater.*, 2012, **11**, 700–709.
5 D. Di Sante, P. Barone, R. Bertacco and S. Picozzi, *Adv. Mater.*, 2013, **25**, 509–513.
6 M. Liebmann, C. Rinaldi, D. Di Sante, J. Kellner, C. Pauly, R. N. Wang, J. E. Boschker, A. Giussani, S. Bertoli, M. Cantoni, L. Baldrati, M. Asa, I. Vobornik, G. Panaccione, D. Marchenko, J. Sánchez-Barriga, O. Rader, R. Calarco, S. Picozzi, R. Bertacco and M. Morgenstern, *Adv. Mater.*, 2016, **28**, 560–565.
7 H. J. Elmers, R. Wallauer, M. Liebmann, J. Kellner, M. Morgenstern, R. N. Wang, J. E. Boschker, R. Calarco, J. Sánchez-Barriga, O. Rader, D. Kutnyakhov, S. V. Chernov, K. Medjanik, C. Tusche, M. Ellguth, H. Volfova, S. Borek,

J. Braun, J. Minár, H. Ebert and G. Schönhense, *Phys. Rev. B*, 2016, **94**, 201403.
8 M. Wuttig and N. Yamada, *Nat. Mater.*, 2007, **6**, 824–832.
9 S. Raoux, W. Wełnic and D. Ielmini, *Chem. Rev.*, 2010, **110**, 240–267.
10 R. E. Simpson, P. Fons, A. V. Kolobov, T. Fukaya, M. Krbal, T. Yagi and J. Tominaga, *Nat. Nanotechnol.*, 2011, **6**, 501–505.
11 S. K. Bahl and K. L. Chopra, *J. Appl. Phys.*, 1970, **41**, 2196–2212.
12 G. Bruns, P. Merkelbach, C. Schlockermann, M. Salinga, M. Wuttig, T. D. Happ, J. B. Philipp and M. Kund, *Appl. Phys. Lett.*, 2009, **95**, 0431081–0431083; S. Roychowdhury, M. Samanta, S. Perumal and K. Biswas, *Chem. Mater.*, 2018, **30**, 5799–5813.
13 E. M. Levin, M. F. Besser and R. Hanus, *J. Appl. Phys.*, 2013, **114**, 083713.
14 S. Perumal, S. Roychowdhury and K. Biswas, *J. Mater. Chem. C*, 2016, **4**, 7520–7536.
15 D. I. Bletskan, *J. Ovonic Res.*, 2005, **1**, 53–60.
16 K. M. Rabe and J. D. Joannopoulos, *Phys. Rev. B: Condens. Matter Mater. Phys.*, 1987, **36**, 6631–6639.
17 Z. Sun, J. Zhou, H.-K. Mao and R. Ahuja, *Proc. Natl. Acad. Sci. U. S. A.*, 2012, **109**, 5948–5952.
18 K. Shportko, S. Kremers, M. Woda, D. Lencer, J. Robertson and M. Wuttig, *Nat. Mater.*, 2008, **7**, 653–658.
19 V. L. Deringer, M. Lumeij and R. Dronskowski, *J. Phys. Chem. C*, 2012, **116**, 15801–15811.
20 P. Nukala, C.-C. Lin, R. Composto and R. Agarwal, *Nat. Commun.*, 2016, **7**, 10482.
21 P. Nukala, R. Agarwal, X. Qian, M. H. Jang, S. Dhara, K. Kumar, A. T. C. Johnson, J. Li and R. Agarwal, *Nano Lett.*, 2014, **14**, 2201–2209.
22 M. A. Hughes, Y. Fedorenko, B. Gholipour, J. Yao, T.-H. Lee, R. M. Gwilliam, K. P. Homewood, S. Hinder, D. W. Hewak, S. R. Elliott and R. J. Curry, *Nat. Commun.*, 2014, **5**, 5346.
23 C. Longeaud, J. Luckas, D. Krebs, R. Carius, J. Klomfass and M. Wuttig, *J. Appl. Phys.*, 2012, **112**, 1137141–1137148.
24 R. Wang, J. E. Boschker, E. Bruyer, D. Di Sante, S. Picozzi, K. Perumal, A. Giussani, H. Riechert and R. Calarco, *J. Phys. Chem. C*, 2014, **118**, 29724–29730.
25 V. Bragaglia, K. Holldack, J. E. Boschker, F. Arciprete, E. Zallo, T. Flissikowski and R. Calarco, *Sci. Rep.*, 2016, **6**, 28560.
26 J.-W. Park, M. Song, S. Yoon, H. Lim, D. S. Jeong, B. Cheong and H. Lee, *Phys. Status Solidi*, 2013, **210**, 267–275.
27 T. Gwon, T. Eom, S. Yoo, H. K. Lee, D. Y. Cho, M. S. Kim, I. Buchanan, M. Xiao, S. Ivanov and C. S. Hwang, *Chem. Mater.*, 2016, **28**, 7158–7166.
28 M. J. Polking, H. Zheng, R. Ramesh and A. P. Alivisatos, *J. Am. Chem. Soc.*, 2011, **133**, 2044–2047.
29 A. C. Jones and M. L. Hitchman, in *Chemical Vapour Deposition: Precursors*, ed. A. C. Jones and M. L. Hitchman, The Royal Society of Chemistry, 2009, pp. 1–36.
30 O. Salicio, C. Wiemer, M. Fanciulli, W. Gawelda, J. Siegel, C. N. Afonso, V. Plausinaitiene and A. Abrutis, *J. Appl. Phys.*, 2009, **105**, 033520.
31 A. Abrutis, V. Plausinaitiene, M. Skapas, C. Wiemer, W. Gawelda, J. Siegel and S. Rushworth, *J. Cryst. Growth*, 2009, **311**, 362–367.
32 I. P. Parkin, L. S. Price, T. G. Hibbert and K. C. Molloy, *J. Mater. Chem.*, 2001, **11**, 1486–1490.
33 K. Ramasamy, V. L. Kuznetsov, K. Gopal, M. A. Malik, J. Raftery, P. P. Edwards and P. O'Brien, *Chem. Mater.*, 2013, **25**, 266–276.
34 S. D. Reid, A. L. Hector, W. Levason, G. Reid, B. J. Waller and M. Webster, *Dalton Trans.*, 2007, 4769–4777; C. Gurnani, S. L. Hawken, A. L. Hector, R. Huang, M. Jura, W. Levason, J. Perkins, G. Reid and G. B. G. Stenning, *Dalton Trans.*, 2018, **47**, 2628–2637.
35 C. H. de Groot, C. Gurnani, A. L. Hector, R. Huang, M. Jura, W. Levason and G. Reid, *Chem. Mater.*, 2012, **24**, 4442–4449.
36 I. Y. Ahmet, M. S. Hill, P. R. Raithby and A. L. Johnson, *Dalton Trans.*, 2018, **47**, 5031–5048.
37 M. F. Davis, W. Levason, G. Reid, M. Webster and W. Zhang, *Dalton Trans.*, 2008, 533–538.
38 G. Gupta, T.-M. Jeong, C. G. Kim and J. Kim, *Mater. Lett.*, 2015, **156**, 121–124.
39 H. S. Kim, E. A. Jung, S. H. Han, J. H. Han, B. K. Park, C. G. Kim and T. M. Chung, *Inorg. Chem.*, 2017, **56**, 4084–4092.
40 T. Chen, W. Hunks, P. S. Chen, G. T. Stauf, T. M. Cameron, C. Xu, A. G. DiPasquale and A. L. Rheingold, *Eur. J. Inorg. Chem.*, 2009, 2047–2049.
41 S. L. Benjamin, C. H. de Groot, A. L. Hector, R. Huang, E. Koukharenko, W. Levason and G. Reid, *J. Mater. Chem. C*, 2015, **3**, 423–430.
42 S. Schlecht and K. Friese, *Eur. J. Inorg. Chem.*, 2003, 1411–1415.
43 P. Bauer Pereira, I. Sergueev, S. Gorsse, J. Dadda, E. Müller and R. P. Hermann, *Phys. Status Solidi B*, 2013, **250**, 1300–1307.
44 T. Chattopadhyay, J. X. Boucherle and H. G. VonSchnering, *J. Phys. C: Solid State Phys.*, 1987, **20**, 1431–1440.
45 S. G. Parker, J. E. Pinnell and L. N. Swink, *J. Mater. Chem.*, 1974, **9**, 1829–1832.
46 A. V. Kolobov, J. Tominaga, P. Fons and T. Uruga, *Appl. Phys. Lett.*, 2003, **82**, 382–384.
47 A. H. Edwards, A. C. Pineda, P. A. Schultz, M. G. Martin, A. P. Thompson, H. P. Hjalmarson and C. J. Umrigar, *Phys. Rev. B: Condens. Matter Mater. Phys.*, 2006, **73**, 045210.
48 G. Kalra and S. Murugavel, *AIP Adv.*, 2015, **5**, 0471271.
49 D. Sarkar, G. Sanjeev and M. G. Mahesha, *Appl. Phys. A: Mater. Sci. Process.*, 2015, **119**, 49–54.
50 M. Upadhyay, S. Murugavel, M. Anbarasu and T. R. Ravindran, *J. Appl. Physiol.*, 2011, **110**, 083711.
51 R. De Bastiani, E. Carria, S. Gibilisco, M. G. Grimaldi, A. R. Pennisi, A. Gotti, A. Pirovano, R. Bez and E. Rimini,

Phys. Rev. B: Condens. Matter Mater. Phys., 2009, **80**, 245205.
52 R. Shaltaf, X. Gonze, M. Cardona, R. K. Kremer and G. Siegle, *Phys. Rev. B: Condens. Matter Mater. Phys.*, 2009, **79**, 075204.
53 S. G. Parker, J. E. Pinnell and L. N. Swink, *J. Mater. Chem.*, 1974, **9**, 1829–1832.
54 ICSD Inorganic Crystal Structure Database Fachinformationszentrum Karlsruhe (FIZ), accessed *via* EPSRC funded National Database Service hosted by the Royal Society of Chemistry.
55 S. Grazulis, D. Chateigner, R. T. Downs, A. F. T. Yokochi, M. Quirós, L. Lutterotti, E. Manakova, J. Butkus, P. Moeck and A. Le Bail, *J. Appl. Crystallogr.*, 2009, **42**, 726–729.